

# Superconducting Transformers

Jan SYKULSKI

Electrical Power Engineering Research Group, School of ECS, University of Southampton, United Kingdom  
Highfield, Southampton, SO17 1BJ, UK

Phone: (+4423) 80593448, fax: (+4423) 80593709, e-mail: [jks@soton.ac.uk](mailto:jks@soton.ac.uk)

**Abstract** — The paper provides an overview of power applications of High Temperature Superconductivity (HTS) with emphasis on superconducting transformers. Properties of available HTS materials are reviewed and modelling aspects briefly introduced. A conceptual design of a 240MVA HTS grid autotransformer is summarised and principal features discussed. The economics of parallel operation is addressed. Finally, details of a small HTS demonstrator built and tested at Southampton University are provided.

**Keywords** — superconducting transformers, high temperature superconductivity, HTS power devices

## I. INTRODUCTION

Recent catastrophic black-outs in New York, London and Italy (August and September 2003) have exposed major vulnerabilities in existing generation, transmission and distribution systems. Severe underinvestment, aging technology and conservatism in the approach to innovation are being blamed and have created a situation where reliability of the entire system is under question. Resources need to be directed into technologies that have the potential to improve the integrity of the system; high temperature superconductivity has such potential. It also has a positive environmental impact by significantly reducing the losses as well as size and weight of the power devices.

The advent of high-temperature superconducting (HTS) materials has renewed interest in the possibilities for superconducting power apparatus offering real economic benefit, within power ratings typical of present system practice. Previously developed low-temperature superconductors (LTS) required cooling by liquid helium to about 4.2K, with advanced cryogenic technology that is expensive both in terms of cost and of refrigeration power expended per unit of heat power removed from the cryostat. The technology for the new materials, which may be based on liquid nitrogen (LN2) at temperatures up to about 78K, is simpler and cheaper, and the ratio of refrigeration power used to heat removed is reduced from over 1000 to about 25. There is significant activity around the world regarding applications of HTS materials to cables, motors, generators, fault current limiters, energy storage devices and transformers. This review builds on the material published previously by the author [1-9] and reflects on the experiences with HTS technology in electrical power applications at the University of Southampton, United Kingdom. Up-to-date information may also be found on a dedicated web page [10].

## II. PROPERTIES OF HTS MATERIALS

The announcement in April 1986, by Muller and Bednorz (IBM) of superconductivity in the perovskite structure Lanthanum-Barium-Copper oxide at 30K, was an important step towards a wider application of superconductivity [11]. This was followed by the discovery of Wu and co-workers in January 1988, of  $Y_1Ba_2Cu_3O_{7-8}$  (YBCO or 123), with a transition temperature of 93K, bringing superconductivity above the boiling point of liquid nitrogen (77.4K at 1Atm), a cheap and widely available cryogen. There has since been much effort on the search for new materials, and the optimization of processes for production of thin films (<1 $\mu$ m), thick films (10-100 $\mu$ m), bulk materials, wires and tapes (Fig. 1) in single or multifilament composites. Many practical problems remain to be solved, but the potential for engineering application is clear.



Figure 1. Multi-filament HTS tape

Unlike LTS materials, HTS superconducting ceramics have highly anisotropic electronic structure, which causes critical current and critical field to have different values on two perpendicular planes. Randomly oriented polycrystalline HTS superconductors have low transport critical current, due not to intrinsic material properties but to misalignment between crystallites and weak superconducting regions at grain boundaries. Alignment or texturing of the material during the process of crystal growth improves properties and can be achieved by various means: temperature gradients, zone melting, two-dimensional configurations, etc.

The most promising known HTS materials for high current applications are given below, with their common numerical reference names in brackets:

Yttrium compounds (YBCO)

$Y_1Ba_2Cu_3O_{7-x}$  (123)  $T_c = 92$  K

$Y_2Ba_4Cu_7O_{15-y}$  (247)  $T_c = 95$  K

Bismuth compounds (BISCCO)

$Bi_2Sr_2Ca_1Cu_2O_y$  (2212)  $T_c = 80$  K

$Bi_{2-x}Pb_xSr_2Ca_2Cu_3O_y$  (2223)  $T_c = 110$  K

Thallium compounds

$(TlPb)_1Sr_2Ca_2Cu_3O_9$  (1223)  $T_c = 120$  K

$Tl_2Ba_2Ca_2Cu_3O_{10}$  (2223)  $T_c = 125$  K

Mercury compounds

$Hg_1Ba_2Ca_2Cu_3O_{10}$  (1223)  $T_c = 153$  K

### III. MODELLING AND SIMULATION

HTS materials exhibit strong flux creep effects [12]. When modelling power loss mechanism due to a flow of alternating current it is therefore not sufficient to use a critical state model [13], which has proved successful when dealing with low temperature superconductors, and it is necessary to consider the flux creep  $E$ - $J$  characteristic. A flux creep region is well described by the Anderson-Kim model [12] in which

$$E = K_1 \sqrt{H} \sinh(K_2 \sqrt{H} J) , \quad (1)$$

where  $K_1$  and  $K_2$  are parameters related to temperature and the properties of the material, or a simpler relationship suggested by Rhyner [14] where

$$E = E_c (J / J_c)^\alpha , \quad \rho = \rho_c (J / J_c)^{\alpha-1} . \quad (2)$$

The critical current density  $J_c$  corresponds to an electric field  $E_c$  of  $100 \mu\text{Vm}^{-1}$ , and  $\rho_c = E_c / J_c$ . The power law (2) contains the linear and critical state extremes ( $\alpha = 1$  and  $\alpha \rightarrow \infty$  respectively). It has been found that for practical HTS materials  $\alpha \approx 20$  and thus the system is very non-linear.

Using the Rhyner model the governing field equation takes the following form in a two-dimensional space

$$\frac{\partial^2 E}{\partial x^2} + \frac{\partial^2 E}{\partial y^2} = \mu_0 \frac{\partial}{\partial t} \left\{ \sigma_c |E|^{\alpha-1} E \right\} , \quad (3)$$

where  $E = E_z / E_c$  for brevity and  $\sigma_c = J_c / E_c$  [6]. Using a rectangular space mesh  $\Delta x \times \Delta y$ , a Finite Difference scheme may be built which yields

$$\left| E_{ij}^{(k+1)} \right|^{\alpha-1} E_{ij}^{(k+1)} = \left| E_{ij}^{(k)} \right|^{\alpha-1} E_{ij}^{(k)} + \Delta t \cdot C_{ij} = K_{ij} , \quad (4)$$

$$E_{ij}^{(k+1)} = \left| K_{ij} \right|^{\alpha-1} K_{ij} . \quad (5)$$

where

$$C = \quad (7)$$

$$\left\{ \mu_0 \sigma_c (\Delta x)^2 \right\}^{-1} \left\{ (E_{i+1,j}^k + E_{i-1,j}^k) + R^2 (E_{i,j+1}^k + E_{i,j-1}^k) - 2(R^2 + 1) E_{i,j}^k \right\}$$

and  $R = \Delta x / \Delta y$ . The indices  $i$  and  $j$  denote the nodal addresses in the  $(x, y)$  space. The loss over a cycle can then be calculated using numerical integration as

$$\int_0^T \int_0^V (J \cdot E) dV dt . \quad (8)$$

The stability requirements for the numerical solution are severe and in order to make the process as fast as possible the time steps are adjusted at each step using the criterion

$$\Delta t \leq \frac{\sigma_c \mu_0 |E|^{\alpha-1} E_c^{1-\alpha}}{2\alpha \left( \frac{1}{\Delta x^2} + \frac{1}{\Delta y^2} \right)} . \quad (9)$$

It has been shown in [6] that field penetration in HTS tapes can be modelled accurately as a highly non-linear diffusion process described above. The knowledge of AC losses is of paramount importance in the design of HTS power devices as these losses are released at low temperature. Figures 2 to 4 show typical results of simulations.

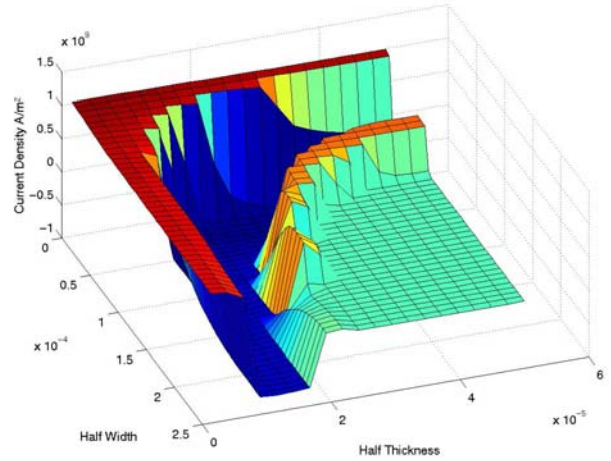


Figure 2. Current density distribution at the instant of a quarter of the maximum current

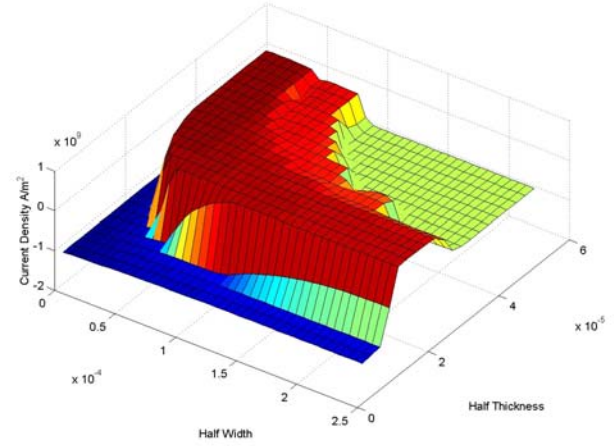


Figure 3. Current density distribution at the instant of max current

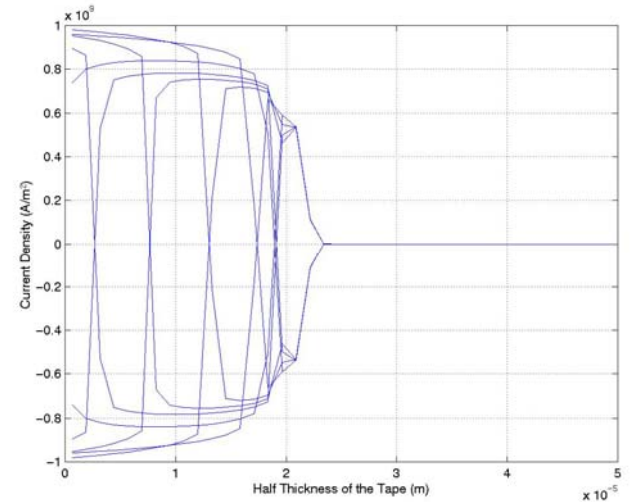


Figure 4. Current density profiles through the tape thickness

The effects of non-linearity have been found to be much stronger than experienced in linear conductors and thus for larger currents (deeper field penetration) the 2D analysis is essential, despite a large aspect ratio of the tape. The analogy with the linear case only works well for smaller currents where a simpler 1D model is quite acceptable.

#### IV. 240MVA GRID AUTOTRANSFORMER

A design feasibility study was conducted for a 240MVA high temperature superconducting grid auto-transformer [1]. The principal feature of the design is the removal of the copper windings and their replacement by HTS equivalents. These are only a fraction (less than 10%) of the bulk of the conventional windings. The inevitable result is windings of reduced mechanical strength, which will stand neither the radial bursting forces nor the axial compressive forces that occur during through-fault conditions without special strengthening structural features. The tap winding is kept outside the cryostat to avoid the heat which could otherwise flow into liquid nitrogen through a large number of connections. With the bulk of the ohmic losses (in common and series windings) removed, it is possible to cope with the core loss and remaining ohmic loss (in the tap windings) by forced gas cooling, leading to an oil-less design of transformer. This has a great advantage of reducing fire risk and environmental hazard from oil spillage. Furthermore, the need for an explosion-proof outer steel tank is removed – though some form of enclosure must be provided for weatherproofing and acoustic noise reduction.

The superconducting windings have small thermal mass and are cryogenically stable (i.e. capable of returning to normal operation after a period of abnormal heating without disconnecting and cooling down) over only a small range of temperature rise. In consequence, the HTS design has very little capability to recover from a through fault without disconnection, in contrast to a conventional transformer. This is the chief weakness of the HTS design; however, the HTS design can *survive* a through fault, though it subsequently needs disconnecting for a period, and there is also good overload capability.

The principal parameters of the suggested transformer design are listed below:

kVA:	240,000
Normal Volts:	400/132 kV
Tappings:	132 kV + 15% - 5% in 14 steps
Line current at normal volts:	346/1054 A
Diagram No:	Yy0 Auto
Guaranteed reactance:	20%
Rated current densities:	
	series winding* = 39.1 A/mm <sup>2</sup>
	common winding* = 36.9 A/mm <sup>2</sup>
	tap winding = 3.0 A/mm <sup>2</sup> (conventional)

(\* average over composite conductor section, comprising both superconducting and matrix materials).

A short summary of the principal features of the HTS design is provided below (based on [1]).

**Core.** Similar to a conventional design, but with leg length and window spans reduced and consequent saving in core weight and overall size.

**Tap change arrangements.** Copper tap windings retained, adjacent to core leg, outside the cryostat, connected to a tap-changer, both of conventional design.

**Cooling of core and tap winding.** Forced-convection gas cooling, probably nitrogen. Gas is forced through axial

ducts to cool the core legs and tap windings. Top and bottom yokes fitted with fibreglass cowling to contain the fanned gas and direct it over yoke surfaces.

**Common and series windings.** Constructed of rectangular section composite conductor comprising about 33% superconducting fibres and 67% matrix metal. The inter-turn insulating tape is applied to one face of the conductor. Individual tapes making up the conductor will be transposed in a normal way. Discs at the high-voltage ends of the series windings interleaved in pairs.

**Winding reinforcement.** Outer diameter of series (high voltage) winding reinforced with fibreglass hoops (possibly pre-stressed) or continuous cylinder. Substantial inner cylinder with multiple spacing sticks supports inside diameter of common winding. Annular clamping plates top and bottom of complete in-cryostat winding assembly, pulled together by eight through-bolts or studs, all constructed of insulating material.

**Cryostats.** One cryostat per leg, each cryostat comprising a vacuum vessel constructed of double-skinned fibreglass, with the vacuum continuously pumped. Cryostat pressure will be slightly in excess of 1 bar, containing nitrogen at 78 K. The intermediate-voltage leads pass through the top lid. High voltage lead passes centrally through cryostat wall.

**Fault and overload capability.** For any substantial through fault, disconnection is required and a period of minutes is needed before reconnecting. Transformer can survive the most severe through fault for about 170 ms, within which time disconnection must be achieved. Internal faults sensed by in-built monitors or terminal voltage and current sensors, which initiate disconnection. Overload capability of 100% is expected.

**Housing.** Oil-less design obviates need for a tank, which is replaced by a steel structure carrying load exerted by bushings. External housing required for weatherproofing, gas-seal for the forced-convection nitrogen coolant and acoustic noise reduction.

Table I summarises the total losses of the HTS transformer design and compares them with the corresponding figures for a conventional 'reference' design. Losses are expressed in percentage form with the total loss in conventional design taken as 100%. Table II shows all the significant global features, covering size and construction as well as performance.

Table I Loss analysis (total loss of conventional design = 100%)

	HTS	Conventional
Core loss	8	9
Clamp stray loss	5	5
Tank loss	-	7
Total copper loss	<1 (tap)	79
Refrigerator power	7	-
Gas-cooling fan loss	2	-
<b>Estimated total loss</b>	<b>23</b>	<b>100</b>

Table II Comparison of technical features

Parameter	HTS	Conventional
Core length*	88.5	100
height*	82.4	100
thickness*	100	100
Window, height* × width*	70 × 78.5	100 × 100
Core weight*	80	100
Winding weight* (common and series)	6.3	100
Tap winding weight*	100	100
Cooling of core and tap winding	forced N2 gas	ONAN/OFAF
Cooling of common and series windings	liquid N2 (with refrigeration plant)	ONAN/OFAF
Guaranteed % reactance	20	20
B in core, T	1.67	1.67
J rated (average of C and S), rms, A/mm <sup>2</sup>	38	2.83
Rated loss, total*	23	100
Overload capability	2 pu, many hours	1.3 pu, 6 hrs 1.5 pu, 30 mins
Through fault capability, pu (+ doubling transient), recovery time without disconnection	2 pu, 64 ms	5 pu, 3s
Survival time at 5 pu (+ doubling transient)	166 ms	seconds (> 3)

(\* shown as percentage of the appropriate value for a conventional transformer)

Table III Cost savings on continuous full-load

Savings/(expenditure)	%
Saving on core plate	1
Saving on continuously transposed copper	7
Saving on copper losses, discount over 10 years	65
Cost of refrigeration plant	-21
First-cost equivalent expenditure on refrigerator drive power, discount over 10 years	-6
Cost of AC conductor, total of 7371 amp-kilometres	-10
<b>Total equivalent first-cost saving</b>	<b>36</b>

(all values are referred to the overall first cost of the conventional transformer, which is taken as 100%)

Table III shows estimates of saving/expenditure components based on continuous operation in rated conditions. It is clear that an expenditure on extra equipment and materials is offset by the enormous value of the saved losses (taken over a 10-year period and discounted at 9.5% per year). However, because of the

redundancy built into the system for security, the load factor of a grid transformer is remarkably low and may be taken as 0.23 average and 0.26 rms. For such load conditions a pessimistic estimate suggests that the total equivalent first-cost saving may now become a net increase of first-cost equivalent expenditure of about 20%.

On the other hand a common practice is to have two transformers fully rated normally connected in parallel. It is thus worth considering an arrangement of an HTS transformer normally connected, in parallel with a conventional transformer normally disconnected but capable of being switched on quickly when required (e.g. during through fault). Hence savings on the losses of the conventional transformer will be very significant. This arrangement is discussed in the next section.

V. PARALLEL OPERATION

Figure 5 shows a typical arrangement of parallel connected transformers. Each transformer is usually rated to take the maximum load on its own, and because that maximum load rarely occurs, the load factor for a typical National Grid transformer in the UK is low, around 23%. A typical probability density function for such a transformer is shown in Fig. 6.

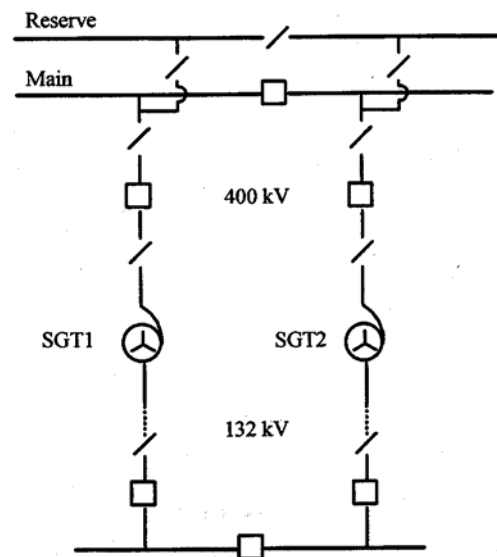


Figure 5. Conventional arrangement of parallel transformers

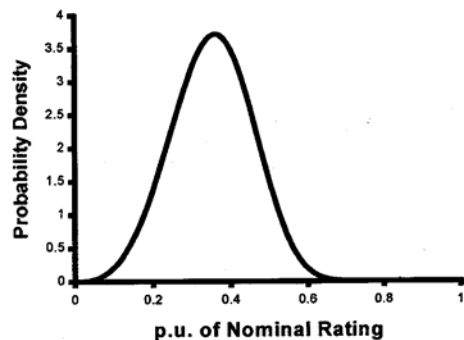


Figure 6. Probability density of load for a typical grid transformer

A suggested scenario is therefore to replace one of the conventional transformers (say SGT1 in Fig. 5) with a HTS “equivalent”. In normal operation the SGT2’s breaker is open and the load passes through SGT1 (HTS). In the event of a through fault, SGT2’s breaker is rapidly closed and SGT1’s opened. This may require faster than usual breakers and associated protection but there is no reason to think that this may not be achieved within the 200ms required. Thus in this configuration it should hardly be necessary to ever use SGT2 (only during faults or maintenance outages) and so it may be possible to de-rate this transformer. The modified probability density distribution is shown in Fig. 7.

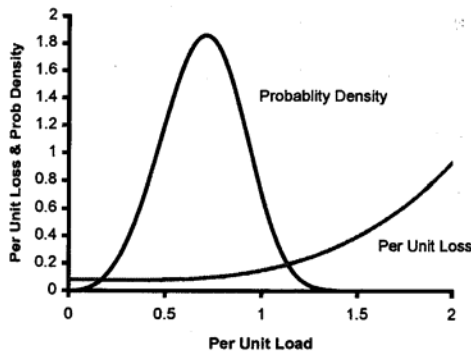


Figure 7. Load probability density and loss as a function of load for a HTS transformer in parallel with a (normally) unconnected conventional unit. The mean load is around 0.7 p.u.

Following the argument put forward in [5], assuming a capital cost of a 240MVA transformer of £1.0M, per unit loss to be 600kW and cost of losses over the transformer life to be £3,000 / kW, we can assess the costs as follows:

Costs (£k)	Superconducting + conventional	2 × conventional
Transformer capital	1,000 + 1,230	2,000
Losses	$0.105 \times 600 \times 3$	$0.426 \times 600 \times 3$
<b>Total</b>	<b>2,419</b>	<b>2,768</b>

This simplistic analysis shows that the combination of HTS and conventional transformer is a lower cost option. Moreover, by inspecting Fig. 7, it is clearly possible to optimise this further by reducing the nominal rating of the HTS transformer thus reducing capital cost. It can be seen that the load would “hardly ever” go much above 1.5 p.u. so the HTS transformer could be of a smaller rating.

## VI. HTS TRANSFORMER DEMONSTRATOR

A small 10kVA HTS demonstrator transformer was designed, built and tested at Southampton University [8, 9]. In order to limit the material cost of this small single-phase unit (predominantly the cost of the superconducting tape), it was decided that the nominal rating at 78K should be 10kVA and only one winding, the secondary, should be superconducting; this also had the benefit of allowing direct comparison of performance between conventional and superconducting windings. The secondary current at this load is 40A. Since the large space required for thermal

insulation between copper and superconducting windings increases the radial flux densities and leakage reactance, a 3 limb construction was used with the two windings on the centre limb. This arrangement minimises both of these problems, and also simplifies the design and construction. It is essential to reduce the radial component of leakage flux in the superconducting winding, as being perpendicular to the face of the tape it is most detrimental to its performance. For example, to carry the peak current of 9.5A per tape, the perpendicular component of peak leakage flux density must be less than 15mT, compared with 110mT for the parallel (axial) component. Field plots with and without the flux diverters are shown in Fig. 8. Flux diverters are placed close to the ends of the superconducting winding in the cryostat and are constructed from low-loss materials to minimise the heat which must be removed from the cryostat.

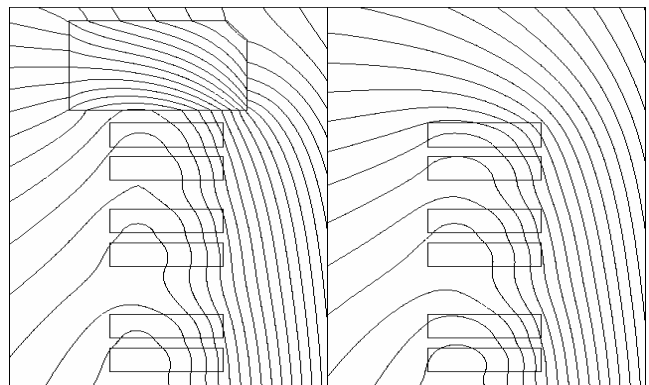


Figure 8. Field plots with and without flux diverters

The flux diverters are made from powdered iron epoxy composite. A small test ring of this material produced a relative permeability of 6, and the 50Hz iron loss at 78K with a peak density of 40mT is less than  $1500\text{W/m}^3$ . This loss is about 25% higher than that at room temperature due to the lower resistivity (the eddy-currents are resistance limited). A more expensive alternative, using flux diverters constructed of segments of ferrite with a relative permeability in excess of 100, was considered. However finite element analysis showed that, although the higher permeability did reduce the radial flux density in the end coils, circulating currents would be more difficult to control. The expected increase in the maximum capacity of the transformer is therefore very small and cannot justify the use of ferrite rings.

Flux diverters have proved to be a very effective means of controlling local field distribution and reducing the winding losses. Figure 9 demonstrates such losses as a function of secondary current. The graph also validates the numerical procedures developed for estimating AC loss in HTS windings described in [7]. The most important observation resulting from these results is that the design requirements differ quite significantly from conventional (that is non-superconducting) transformers where the local shape of leakage field would not have mattered, whereas for the HTS winding a two-fold reduction of loss has been achieved. This emphasises the importance of very careful field modelling using finite element or similar software.

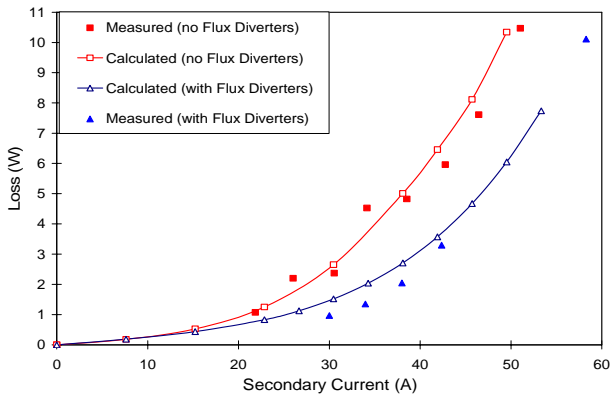


Figure 9. Measured / calculated losses with and without flux diverters

The BPSCCO-2223 tape of the HTS winding (Fig. 10) has 37 filaments in a silver matrix of outer dimensions  $3.72 \times 0.24 \text{ mm}$ . The nominal critical current in zero applied field at 78K is 20A, giving a bulk critical current density of  $22.4 \text{ A/mm}^2$ . Each 28-turn disc consists of two tapes in each layer. There are nine discs and so 18 half-discs are available to form the six parallel paths required to carry the secondary current in the presence of the leakage field.

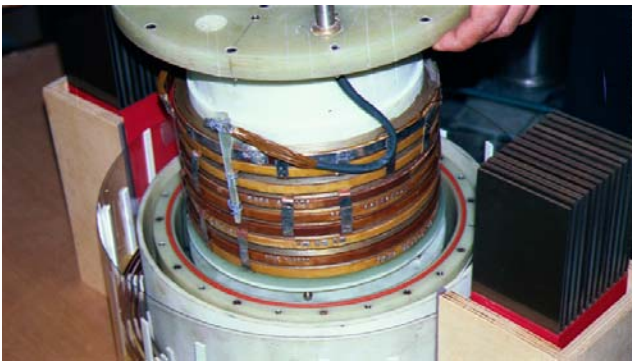


Figure 10. HTS winding of the 10kVA demonstrator

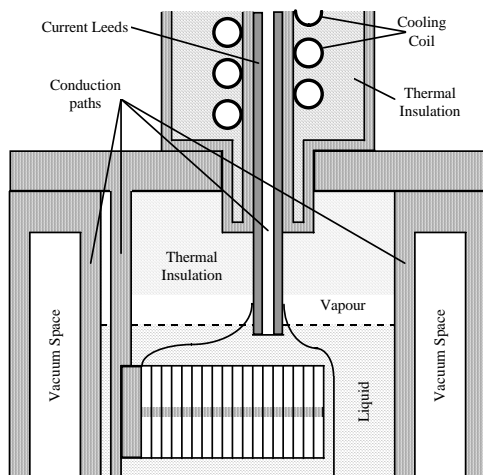


Figure 11. The cryostat and current leads

The epoxy-filled fibre-glass cryostat (Fig. 11) consists of an inner annulus – which contains the HTS winding and liquid nitrogen – fitting inside the outer annulus. The cavity between the two halves is filled with superinsulation and evacuated to form the thermal insulation around the inner cryostat. The whole assembly is threaded by the

centre limb of the transformer laminated core. The complicated shape of the cryostat is necessary because it is not feasible to operate with a “cold” core in view of the loss of nitrogen that would be caused by the iron losses. Neither can the cryostat be made of electrically conducting material because it would act as a short-circuited turn.

## VII. CONCLUSIONS

High Temperature Superconductivity has great potential in electric power applications (generators, motors, fault current limiters, transformers, flywheels, cables, etc.) as losses and sizes of devices are significantly reduced. The technology is now mature and prototypes are considered. The ability to predict and reduce all ‘cold’ losses is crucial to show economic advantages of HTS designs.

## REFERENCES

- [1] Sykulski J.K. et al – *High Temperature Superconducting Power Transformers: Conclusions from a Design Study* – IEE Proceedings: Electrical Power Applications, vol. 146, no 1, pp. 41-52, January 1999.
- [2] Ship K.S., Goddard K.F. and Sykulski J.K. – *Field optimisation in a synchronous generator with high temperature superconducting field winding and magnetic core* – IEE Proceedings (Science, Measurement and Technology), vol. 149, no 5, pp. 194-198, 2002.
- [3] Ship K. S. and Sykulski J.K. – *Field modelling and optimisation of a high temperature superconducting synchronous generator with a coreless rotor* – Fifth IEE International Conference on Computation in Electromagnetics, pp. 109-110, 2004. ISSN 0537-9989
- [4] Sykulski J.K. – *Applications of High Temperature Superconductivity in Electrical Power Devices: the Southampton perspective* – Proceedings of Superconductivity UK, IEE Savoy Place, London, 2003.
- [5] Sykulski J.K. et al – *The design, construction and operation of high temperature superconducting transformers: practical considerations* – Proceedings of 38th Session of the Int Conference on Large High Voltage Electric Systems (CIGRE), Paris, no 12-203, 27 Aug - 1 Sept 2000.
- [6] Sykulski J.K. et al – *2D modelling of field diffusion and AC losses in high temperature superconducting tapes* – IEEE Transactions on Magnetic, vol. 36, no 4, pp. 1178-82, 2000.
- [7] Sykulski J.K., Goddard K.F. and Stoll R.L. – *A method of estimating the total AC loss in a high-temperature superconducting transformer winding* – IEEE Transactions on Magnetic, vol. 36, no 4, pp. 1183-7, 2000.
- [8] Sykulski J.K. et al – *Design of a HTS demonstrator transformer* – Institute of Physics Publ., pp. 571-4, 1999.
- [9] Sykulski J.K. et al – *High temperature superconducting demonstrator transformer: design considerations and first test results* – IEEE Transactions on Magnetics, vol. 35, no 5, pp. 3559-61, 1999.
- [10] <http://www.superconductors.org/>
- [11] Muller K.A. and Bednorz J.G. – *Possible high Tc superconductivity in the Ba-La-Cu-O system* – J. Phys., B, vol. 64, pp. 405-407, 1986.
- [12] Anderson P.W. – *Theory of flux creep in hard superconductors* – Phys. Rev. Lett., vol. 9, pp. 309-311, 1962.
- [13] Bean C.P. – *Magnetization of high-field superconductors* – Rev. Mod. Phys., vol. 36, pp. 31-39, 1964.
- [14] Rhyner J. – *Magnetic properties and ac losses of superconductors with power law current-voltage characteristics* – Physica C, vol. 212, pp. 292-300, 1993.